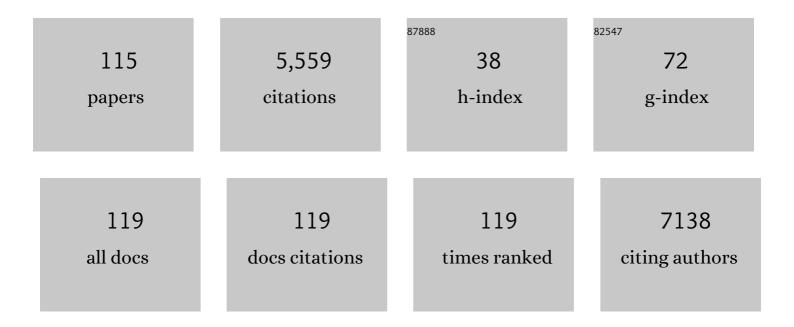
List of Publications by Year in descending order

Source: https://exaly.com/author-pdf/3416531/publications.pdf Version: 2024-02-01



#	Article	IF	CITATIONS
1	Transition-metal doped titanate nanowire photocatalysts boosted by selective ion-exchange induced defect engineering. Applied Surface Science, 2022, 591, 153116.	6.1	10
2	lon selective nano-mesh electrode for long-term continuous monitoring of wastewater quality fabricated using template-guided membrane immobilization. Environmental Science: Nano, 2022, 9, 2149-2160.	4.3	5
3	Solvent effects on the heterogeneous growth of TiO2 nanostructure arrays by solvothermal synthesis. Catalysis Today, 2021, 360, 275-283.	4.4	27
4	Mass transport in nanoarray monolithic catalysts: An experimental-theory study. Chemical Engineering Journal, 2021, 405, 126906.	12.7	16
5	NiO nanosheet array integrated monoliths for low temperature catalytic propane oxidation: A study on the promotion effect of Ce doping. Catalysis Today, 2021, 360, 194-203.	4.4	6
6	Synergistic catalysis by Mn promoted ceria for molecular oxygen assisted epoxidation. Applied Catalysis B: Environmental, 2021, 282, 119573.	20.2	39
7	Single Chemical Sensor for Multi-Analyte Mixture Detection and Measurement: A Review. Selected Topics in Electornics and Systems, 2021, , 67-82.	0.2	0
8	Low-Concentration NO <i>_x</i> Gas Analysis Using Single Bimodular ZnO Nanorod Sensor. ACS Sensors, 2021, 6, 2979-2987.	7.8	19
9	Signal Generation, Acquisition, and Processing in Brain Machine Interfaces: A Unified Review. Frontiers in Neuroscience, 2021, 15, 728178.	2.8	9
10	Laser sintering method induced c-axis growth of Mg0.2Zn0.8O nano-film for ultraviolet photodetector. Journal of Materials Science: Materials in Electronics, 2020, 31, 505-510.	2.2	4
11	Polymerâ€Assisted Coâ€Assembly towards Synthesis of Mesoporous Titania Encapsulated Monodisperse PdAu for Highly Selective Hydrogenation of Phenylacetylene. ChemCatChem, 2020, 12, 1476-1482.	3.7	8
12	Solar-driven efficient methane catalytic oxidation over epitaxial ZnO/La0.8Sr0.2CoO3 heterojunctions. Applied Catalysis B: Environmental, 2020, 265, 118469.	20.2	44
13	Self-limiting growth of ligand-free ultrasmall bimetallic nanoparticles on carbon through under temperature reduction for highly efficient methanol electrooxidation and selective hydrogenation. Applied Catalysis B: Environmental, 2020, 264, 118553.	20.2	20
14	In Situ Microscopy Study of ZnO Acid Etching Nanostructures. Microscopy and Microanalysis, 2020, 26, 1464-1466.	0.4	0
15	Nanoarray-Based Monolithic Adsorbers for SO2 Removal. Emission Control Science and Technology, 2020, 6, 315-323.	1.5	3
16	Multiâ€Gas Sensing: Single Bimodular Sensor for Differentiated Detection of Multiple Oxidative Gases (Adv. Mater. Technol. 7/2020). Advanced Materials Technologies, 2020, 5, 2070042.	5.8	0
17	Toward Long-Term Accurate and Continuous Monitoring of Nitrate in Wastewater Using Poly(tetrafluoroethylene) (PTFE)–Solid-State Ion-Selective Electrodes (S-ISEs). ACS Sensors, 2020, 5, 3182-3193.	7.8	39
18	Tailoring two-dimensional nanomaterials by structural engineering for chemical and biological sensing. Sensors and Actuators Reports, 2020, 2, 100024.	4.4	8

#	Article	IF	CITATIONS
19	Single Bimodular Sensor for Differentiated Detection of Multiple Oxidative Gases. Advanced Materials Technologies, 2020, 5, 1901152.	5.8	2
20	Perovskite-sensitized β-Ga ₂ O ₃ nanorod arrays for highly selective and sensitive NO ₂ detection at high temperature. Journal of Materials Chemistry A, 2020, 8, 10845-10854.	10.3	21
21	Antiferromagnetic and dielectric behavior in polycrystalline GdFe0.5Cr0.5O3 thin film. APL Materials, 2020, 8, 031106.	5.1	9
22	Activating low-temperature diesel oxidation by single-atom Pt on TiO2 nanowire array. Nature Communications, 2020, 11, 1062.	12.8	90
23	Hierarchical and scalable integration of nanostructures for energy and environmental applications: a review of processing, devices, and economic analyses. Nano Futures, 2020, 4, 012002.	2.2	12
24	Elucidating the Nature of the Cu(I) Active Site in CuO/TiO ₂ for Excellent Low-Temperature CO Oxidation. ACS Applied Materials & amp; Interfaces, 2020, 12, 7091-7101.	8.0	51
25	Enhancing ZnO nanowire gas sensors using Au/Fe ₂ O ₃ hybrid nanoparticle decoration. Nanotechnology, 2020, 31, 325505.	2.6	7
26	Single Chemical Sensor for Multi-Analyte Mixture Detection and Measurement: A Review. International Journal of High Speed Electronics and Systems, 2020, 29, 2040008.	0.7	0
27	High resolution air flow velocity monitoring using air flow resistance-type sensor film (AFRSF). Sensors and Actuators A: Physical, 2019, 297, 111562.	4.1	3
28	Alkali-metal poisoning effect of total CO and propane oxidation over Co3O4 nanocatalysts. Applied Catalysis B: Environmental, 2019, 256, 117859.	20.2	78
29	Microwave-assisted integration of transition metal oxide nanocoatings on manganese oxide nanoarray monoliths for low temperature CO oxidation. Applied Catalysis B: Environmental, 2019, 255, 117766.	20.2	32
30	lon-Exchange Loading Promoted Stability of Platinum Catalysts Supported on Layered Protonated Titanate-Derived Titania Nanoarrays. ACS Applied Materials & Interfaces, 2019, 11, 21515-21525.	8.0	10
31	Metal Oxide Nanoarrays for Chemical Sensing: A Review of Fabrication Methods, Sensing Modes, and Their Inter-correlations. Frontiers in Materials, 2019, 6, .	2.4	47
32	Reactive sites rich porous tubular yolk-shell g-C3N4 via precursor recrystallization mediated microstructure engineering for photoreduction. Applied Catalysis B: Environmental, 2019, 253, 196-205.	20.2	91
33	Robust and well-controlled TiO ₂ –Al ₂ O ₃ binary nanoarray-integrated ceramic honeycomb for efficient propane combustion. CrystEngComm, 2019, 21, 2727-2735.	2.6	5
34	Multiple strategies to decrease ignition temperature for soot combustion on ultrathin MnO2- nanosheet array. Applied Catalysis B: Environmental, 2019, 246, 312-321.	20.2	77
35	Ceria-based nanoflake arrays integrated on 3D cordierite honeycombs for efficient low-temperature diesel oxidation catalyst. Applied Catalysis B: Environmental, 2019, 245, 623-634.	20.2	28
36	High performance diesel oxidation catalysts using ultra-low Pt loading on titania nanowire array integrated cordierite honeycombs. Catalysis Today, 2019, 320, 2-10.	4.4	28

#	Article	IF	CITATIONS
37	Pre-surface leached cordierite honeycombs for MnxCo3-xO4 nano-sheet array integration with enhanced hydrocarbons combustion. Catalysis Today, 2019, 320, 196-203.	4.4	26
38	Mesoporous Perovskite Nanotubeâ€Array Enhanced Metallicâ€6tate Platinum Dispersion for Low Temperature Propane Oxidation. ChemCatChem, 2018, 10, 2184-2189.	3.7	14
39	Methanol Production: Cuâ€Decorated ZnO Nanorod Array Integrated Structured Catalysts for Lowâ€Pressure CO ₂ Hydrogenation to Methanol (Adv. Mater. Interfaces 3/2018). Advanced Materials Interfaces, 2018, 5, 1870011.	3.7	3
40	Boosting catalytic propane oxidation over PGM-free Co3O4 nanocrystal aggregates through chemical leaching: A comparative study with Pt and Pd based catalysts. Applied Catalysis B: Environmental, 2018, 226, 585-595.	20.2	113
41	Quasi free K cations confined in hollandite-type tunnels for catalytic solid (catalyst)-solid (reactant) oxidation reactions. Applied Catalysis B: Environmental, 2018, 232, 108-116.	20.2	85
42	Cuâ€Decorated ZnO Nanorod Array Integrated Structured Catalysts for Lowâ€Pressure CO ₂ Hydrogenation to Methanol. Advanced Materials Interfaces, 2018, 5, 1700730.	3.7	20
43	Direct Synthesis of Conformal Layered Protonated Titanate Nanoarray Coatings on Various Substrate Surfaces Boosted by Low-Temperature Microwave-Assisted Hydrothermal Synthesis. ACS Applied Materials & Interfaces, 2018, 10, 35164-35174.	8.0	10
44	Nanostructured TiO2 Support Effect on Hydrothermal Stability of Platinum based Catalysts. Microscopy and Microanalysis, 2018, 24, 1642-1643.	0.4	7
45	Copper manganese oxide enhanced nanoarray-based monolithic catalysts for hydrocarbon oxidation. Journal of Materials Chemistry A, 2018, 6, 19047-19057.	10.3	35
46	Template-Guided Programmable Janus Heteronanostructure Arrays for Efficient Plasmonic Photocatalysis. Nano Letters, 2018, 18, 4914-4921.	9.1	42
47	Rational design, synthesis and evaluation of ZnO nanorod array supported Pt:La0.8Sr0.2MnO3 lean NOx traps. Applied Catalysis B: Environmental, 2018, 236, 348-358.	20.2	22
48	UV-enhanced CO sensing using Ga2O3-based nanorod arrays at elevated temperature. Applied Physics Letters, 2017, 110, .	3.3	36
49	Scalable Integration of Highly Uniform Mn _{<i>x</i>} Co _{3â^'<i>x</i>} O ₄ Nanosheet Array onto Ceramic Monolithic Substrates for Lowâ€Temperature Propane Oxidation. ChemCatChem, 2017, 9, 4112-4119.	3.7	36
50	Band structure engineering strategies of metal oxide semiconductor nanowires and related nanostructures: A review. Semiconductor Science and Technology, 2017, 32, 073001.	2.0	18
51	Understanding low temperature oxidation activity of nanoarray-based monolithic catalysts: from performance observation to structural and chemical insights. Emission Control Science and Technology, 2017, 3, 18-36.	1.5	18
52	Stress-Induced Shift of Band Gap in ZnO Nanowires from Finite-Element Modeling. Physical Review Applied, 2017, 8, .	3.8	7
53	Scalable continuous flow synthesis of ZnO nanorod arrays in 3-D ceramic honeycomb substrates for low-temperature desulfurization. CrystEngComm, 2017, 19, 5128-5136.	2.6	16
54	Nano-Array Integrated Structured Catalysts: A New Paradigm upon Conventional Wash-Coated Monolithic Catalysts?. Catalysts, 2017, 7, 253.	3.5	18

#	Article	IF	CITATIONS
55	Nano-array integrated monolithic devices: toward rational materials design and multi-functional performance by scalable nanostructures assembly. CrystEngComm, 2016, 18, 2980-2993.	2.6	23
56	Perovskite Nanoparticle-Sensitized Ga ₂ O ₃ Nanorod Arrays for CO Detection at High Temperature. ACS Applied Materials & Interfaces, 2016, 8, 8880-8887.	8.0	65
57	Nanowire Array Structures for Photocatalytic Energy Conversion and Utilization: A Review of Design Concepts, Assembly and Integration, and Function Enabling. Advanced Energy Materials, 2016, 6, 1600683.	19.5	89
58	Nanostructured cerium oxide: preparation, characterization, and application in energy and environmental catalysis. MRS Communications, 2016, 6, 311-329.	1.8	59
59	Ni- and Mn-Promoted Mesoporous Co ₃ O ₄ : A Stable Bifunctional Catalyst with Surface-Structure-Dependent Activity for Oxygen Reduction Reaction and Oxygen Evolution Reaction. ACS Applied Materials & Interfaces, 2016, 8, 20802-20813.	8.0	191
60	Tunable UV response and high performance of zinc stannate nanoparticle film photodetectors. Journal of Materials Chemistry C, 2016, 4, 6176-6184.	5.5	32
61	Manganese Oxide Nanoarray-Based Monolithic Catalysts: Tunable Morphology and High Efficiency for CO Oxidation. ACS Applied Materials & amp; Interfaces, 2016, 8, 7834-7842.	8.0	73
62	Low temperature propane oxidation over Co3O4 based nano-array catalysts: Ni dopant effect, reaction mechanism and structural stability. Applied Catalysis B: Environmental, 2016, 180, 150-160.	20.2	174
63	ZnO/perovskite core–shell nanorod array based monolithic catalysts with enhanced propane oxidation and material utilization efficiency at low temperature. Catalysis Today, 2015, 258, 549-555.	4.4	35
64	Nano-array based monolithic catalysts: Concept, rational materials design and tunable catalytic performance. Catalysis Today, 2015, 258, 441-453.	4.4	48
65	Bimodular high temperature planar oxygen gas sensor. Frontiers in Chemistry, 2014, 2, 57.	3.6	8
66	Controlled synthesis and structure tunability of photocatalytically active mesoporous metal-based stannate nanostructures. Applied Surface Science, 2014, 296, 53-60.	6.1	24
67	Highly efficient visible-light driven photocatalysts: a case of zinc stannate based nanocrystal assemblies. Journal of Materials Chemistry A, 2014, 2, 4157-4167.	10.3	40
68	A review of helical nanostructures: growth theories, synthesis strategies and properties. Nanoscale, 2014, 6, 9366.	5.6	123
69	Monolithically Integrated Spinel M _{<i>x</i>} Co _{3â^'<i>x</i>} O ₄ (M=Co, Ni, Zn) Nanoarray Catalysts: Scalable Synthesis and Cation Manipulation for Tunable Lowâ€Temperature CH ₄ and CO Oxidation. Angewandte Chemie - International Edition, 2014, 53. 7223-7227.	13.8	170
70	Mechanical-Agitation-Assisted Growth of Large-Scale and Uniform ZnO Nanorod Arrays within 3D Multichannel Monolithic Substrates. Crystal Growth and Design, 2013, 13, 3657-3664.	3.0	27
71	Single crystalline brookite titanium dioxide nanorod arrays rooted on ceramic monoliths: a hybrid nanocatalyst support with ultra-high surface area and thermal stability. CrystEngComm, 2013, 15, 8345.	2.6	19
72	Nonprecious catalytic honeycombs structured with three dimensional hierarchical Co3O4 nano-arrays for high performance nitric oxide oxidation. Journal of Materials Chemistry A, 2013, 1, 9897.	10.3	73

#	Article	IF	CITATIONS
73	Robust 3-D configurated metal oxide nano-array based monolithic catalysts with ultrahigh materials usage efficiency and catalytic performance tunability. Nano Energy, 2013, 2, 873-881.	16.0	76
74	Hierarchically nanostructured materials for sustainable environmental applications. Frontiers in Chemistry, 2013, 1, 18.	3.6	62
75	Hierarchical Assembly of Multifunctional Oxide-based Composite Nanostructures for Energy and Environmental Applications. International Journal of Molecular Sciences, 2012, 13, 7393-7423.	4.1	37
76	Direct Synthesis of ZnO Nanorod Field Emitters on Metal Electrodes. Crystal Growth and Design, 2012, 12, 5051-5055.	3.0	10
77	In situ TPR removal: a generic method for fabricating tubular array devices with mechanical and structural soundness, and functional robustness on various substrates. Journal of Materials Chemistry, 2012, 22, 23098.	6.7	14
78	La0.67Sr0.33MnO3 nanofibers for in situ, real-time, and stable high temperature oxygen sensing. RSC Advances, 2012, 2, 3872.	3.6	19
79	CeO2 nanofibers for in situ O2 and CO sensing in harsh environments. RSC Advances, 2012, 2, 5193.	3.6	51
80	Three dimensional koosh ball nanoarchitecture with a tunable magnetic core, fluorescent nanowire shell and enhanced photocatalytic property. Journal of Materials Chemistry, 2012, 22, 6862.	6.7	22
81	Lowâ€Field Magnetoresistance in La _{0.67} Sr _{0.33} MnO ₃ :ZnO Composite Film. Advanced Functional Materials, 2012, 22, 3591-3595.	14.9	45
82	Synthesis, characterization and CO oxidation of TiO2/(La,Sr)MnO3 composite nanorod array. Catalysis Today, 2012, 184, 178-183.	4.4	27
83	Synthesis and Thermal Degradation of Fire-Retardant Zinc Hydroxystannate Nanocube Coated Textiles. Science of Advanced Materials, 2012, 4, 819-824.	0.7	2
84	Conversion of Functional Nanofilm Into Nanostructures Using Combination of <i>In-Situ</i> Carbothermal and Stress Induced Recrystallization. Science of Advanced Materials, 2012, 4, 837-842.	0.7	2
85	<i>A Special Issue</i> on Advanced Nanomaterials: Manufacturing and Processing. Science of Advanced Materials, 2012, 4, 781-783.	0.7	0
86	Thermal oxidation of Cu nanofilm on three-dimensional ZnO nanorod arrays. Journal of Materials Chemistry, 2011, 21, 9564.	6.7	18
87	Synthesis of tin nanodendrites via galvanic replacement reaction and their thermal conversion to nanodendritic tin oxide for ultrasensitive electrochemical sensing. RSC Advances, 2011, 1, 1500.	3.6	8
88	Structure and magnetic properties of three-dimensional (La,Sr)MnO3 nanofilms on ZnO nanorod arrays. Applied Physics Letters, 2011, 98, 123105.	3.3	32
89	Conversion of [0001] Textured ZnO Nanofilm into [011Ì0] Directed Nanowires Driven by CO Adsorption: In Situ Carbothermal Synthesis and Complementary First Principles Thermodynamics Simulations. Journal of Physical Chemistry C, 2011, 115, 7372-7376.	3.1	2
90	A review of NOx storage/reduction catalysts: mechanism, materials and degradation studies. Catalysis Science and Technology, 2011, 1, 552.	4.1	196

#	Article	IF	CITATIONS
91	Morphology and phase selective synthesis of CuxO (x=1, 2) nanostructures and their catalytic degradation activity. Materials Science and Engineering B: Solid-State Materials for Advanced Technology, 2010, 166, 113-117.	3.5	19
92	(La,Sr)CoO3/ZnO nanofilm–nanorod diode arrays for photo-responsive moisture and humidity detection. Journal Physics D: Applied Physics, 2010, 43, 272002.	2.8	15
93	Annealing induced nanostructure and photoluminescence property evolution in solution-processed Mg-alloyed ZnO nanowires. Applied Physics Letters, 2010, 97, .	3.3	23
94	Surface Dezincification and Selective Oxidation Induced Heterogeneous Semiconductor Nanowire/Nanofilm Network Junctions. Crystal Growth and Design, 2010, 10, 3942-3948.	3.0	6
95	Carbon-assisted lateral self-assembly of amorphous silica nanowires. CrystEngComm, 2010, 12, 2817.	2.6	14
96	Oxide-catalyzed growth of Ag2O/Zn2SnO4 hybrid nanowires and their reversible catalytic ambient ethanol/oxygen detection. Journal of Materials Chemistry, 2010, 20, 5265.	6.7	9
97	Gas adsorption and high-emission current induced degradation of field emission characteristics in solution-processed ZnO nanoneedles. Journal of Applied Physics, 2010, 108, 124318.	2.5	9
98	Isothermal Gas Flow Separation of Helical ZnS Nanowires and Straight Nanobelts. Science of Advanced Materials, 2010, 2, 421-427.	0.7	5
99	Low temperature synthesis and characterization of MgO/ZnO composite nanowire arrays. Nanotechnology, 2009, 20, 125608.	2.6	64
100	Spherical CuO synthesized by a simple hydrothermal reaction: Concentration-dependent size and its electrocatalytic application. Materials Research Bulletin, 2009, 44, 1681-1686.	5.2	73
101	Zigzag zinc blende ZnS nanowires: Large scale synthesis and their structure evolution induced by electron irradiation. Nano Research, 2009, 2, 966-974.	10.4	13
102	Seedless Synthesis and Thermal Decomposition of Single Crystalline Zinc Hydroxystannate Cubes. Crystal Growth and Design, 2009, 9, 4456-4460.	3.0	42
103	Synthesis, characterization, and photocatalytic properties of ZnO/(La,Sr)CoO3 composite nanorod arrays. Journal of Materials Chemistry, 2009, 19, 970.	6.7	75
104	Electronic Transport in Superlattice-Structured ZnO Nanohelix. Nano Letters, 2009, 9, 137-143.	9.1	72
105	Vertically aligned ZnO nanowire arrays on GaN and SiC substrates. Chemical Physics Letters, 2008, 460, 253-256.	2.6	40
106	Bridged ZnO nanowires across trenched electrodes. Applied Physics Letters, 2007, 91, 142108.	3.3	33
107	Multicolored ZnO Nanowire Architectures on Trenched Silicon Substrates. Journal of Physical Chemistry C, 2007, 111, 13763-13769.	3.1	16
108	Direct synthesis and structure characterization of ultrafine CeO2nanoparticles. Nanotechnology, 2006, 17, 5983-5987.	2.6	159

#	Article	IF	CITATIONS
109	ZnO Nanobelt/Nanowire Schottky Diodes Formed by Dielectrophoresis Alignment across Au Electrodes. Nano Letters, 2006, 6, 263-266.	9.1	342
110	SiC-Shell Nanostructures Fabricated by Replicating ZnO Nano-objects: A Technique for Producing Hollow Nanostructures of Desired Shape. Small, 2006, 2, 1344-1347.	10.0	38
111	Nanowire as pico-gram balance at workplace atmosphere. Solid State Communications, 2006, 139, 222-226.	1.9	42
112	Single-Crystal Hexagonal Disks and Rings of ZnO: Low-Temperature, Large-Scale Synthesis and Growth Mechanism. Angewandte Chemie - International Edition, 2004, 43, 5238-5242.	13.8	455
113	Perfect Orientation Ordered in-Situ One-Dimensional Self-Assembly of Mn-Doped PbSe Nanocrystals. Journal of the American Chemical Society, 2004, 126, 14816-14821.	13.7	132
114	Measuring the Work Function at a Nanobelt Tip and at a Nanoparticle Surface. Nano Letters, 2003, 3, 1147-1150.	9.1	257
115	Self-Assembled Nanowireâ^'Nanoribbon Junction Arrays of ZnO. Journal of Physical Chemistry B, 2002, 106, 12653-12658.	2.6	327